

Long-term meter wavelength variability study of Blazar J1415+1320 using the Ooty Radio Telescope

SRAVANI.VADDI,^{1,2} P.K. MANOHARAN,^{1,2} AND ANISH ROSHI^{1,2}

¹*Arecibo Observatory, Arecibo, Puerto Rico, USA*

²*University of Central Florida, Orlando, USA*

ABSTRACT

We present light curve for J1415+1320 blazar monitored at 327 MHz using the Ooty Radio Telescope from the period 1989 to 2018. The source displayed variability more than 5σ value above its mean flux density (2.70 ± 0.02 Jy) at two epochs around 2008 and 2009. Here σ is the RMS variation of the flux density over the epoch. The variability analysis techniques indicate weak variability but inadequate to quantify if it is due to an intrinsic or extrinsic mechanism.

Keywords: Blazar – Radio astronomy –

1. INTRODUCTION

J1415+1320, a BL Lac has alluded the astronomers from a very long time owing to its controversial properties. Some of these properties include (a) apparent yet rare association of the AGN with an optical spiral host (McHardy et al. 1994), (b) detection of a counter jet in a blazar type AGN (Perlman et al. 1994), (c) its association to the class of compact symmetric objects as well as blazar (Wilkinson et al. 1994; Perlman et al. 1996), (d) strong variability in radio light curve attributed to both relativistic beaming and gravitational lensing (Vedantham et al. 2017). Some of these controversies have been addressed in Readhead et al. (2021) and conclude that J1415+1320 is actually a background object in the redshift range $0.247 < z < 0.5$ and is not associated with the previously known spiral host.

Variability in an AGN reveals crucial information on the size, structure, and dynamics of the radiating source down to scales that otherwise need extremely long baseline interferometers. While variability in a source is a complicated feature that has not yet been fully understood, several possible mechanisms have been discussed in the literature broadly categorized into intrinsic and extrinsic phenomenon. Variability due to an intrinsic phenomenon occur due to, but not limited to, – (a) shocks waves forming and propagating relativistically along the jets (Marscher & Gear 1985; Aller et al. 1985; Qian et al. 1991), (b) magnetohydrodynamic instabili-

ties in the jet (Marscher 2014), (c) relativistic beaming due to changes in the viewing angle in a twisted/bent jet (Raiteri et al. 2017) (d) magnetic reconnection in turbulent jets (Sironi et al. 2015; Werner et al. 2016). Variability is also observed owing to extrinsic phenomenon such as refractive interstellar scintillation caused by large-scale irregularities in the ISM (Quirrenbach et al. 1992).

Owing to the peculiar behaviour of J1415+1320, extensive radio monitoring has been done by numerous telescopes and at various frequencies. Figure 1 shows the radio light curve spanning nearly 40 years and at several frequencies ranging from 327 MHz to 350 GHz. The data has been compiled from various monitoring programs found in the literature. The source exhibits variability at all frequencies. Strong variability is seen at high frequencies compared to low frequencies. The variability features seen at 15 GHz are followed at 8 and 5 GHz albeit at a low level. Further, within the high frequencies, the strength of variability decreased over time. Most of the monitoring is done at > 2 GHz; we present in this article, long-term, low frequency 327 MHz flux density observations of J1415+1320 taken using Ooty Radio Telescope (Swarup et al. 1971).

2. DATA

The data for this study comes from the extensive interplanetary scintillation (IPS) database¹ collected during the period 1989–2018 on a large number of compact radio sources of angular size less than 250 mas from the

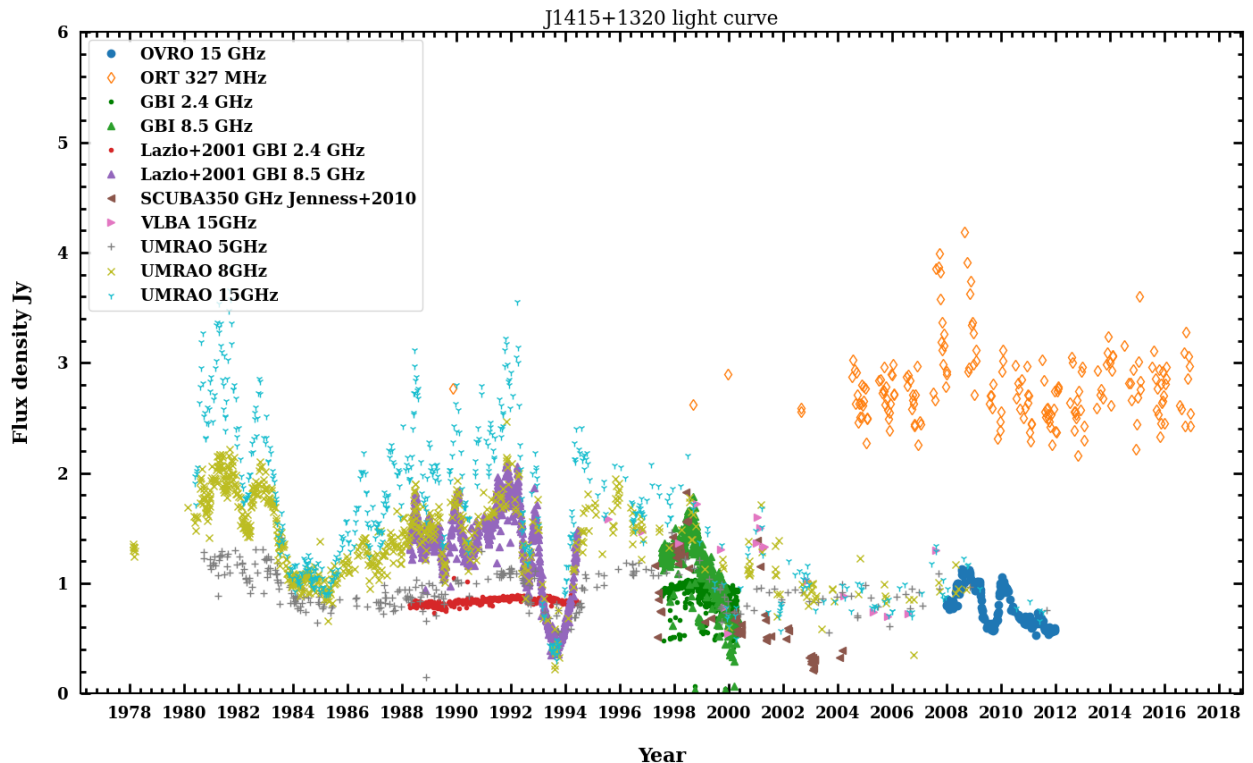


Figure 1. Radio light curve of J1415+1320 at different frequencies.

Ooty Radio Telescope (ORT), operated by the Radio Astronomy Centre, Tata Institute of Fundamental Research, India, at 327 MHz (Swarup et al. 1971). The main purpose of these IPS observations, obtained routinely on hundreds of radio sources per day, were to investigate the three-dimensional distributions of the solar wind density turbulence and speed at short time intervals of a few days as well as at different phases of solar activity (e.g. Manoharan 2012; Manoharan et al. 2017). The IPS measurements on each source were made within the solar elongation range of about $\varepsilon \approx \pm 60$ degree with respect to the Sun, which spanned over an observing period of about 4-month and enabled the study of heliocentric distance dependence of the properties of the solar wind. Typically a source was observed for about 2–3 min and the same source was likely observed more than once in a day at different hour-angle positions. Everyday observation also included several flux density calibrators distributed almost uniformly between the start and end of each observing session.

In this study, the above large IPS database from the ORT has been employed to study the variation of the total flux density of BL Lac object J1415+1320 over many years. The data is made available online in Vizier.

3. RESULTS

Figure 2 displays the flux density of J1415+1320 from the ORT at 327 MHz in the time period between 1989.8 and 2017. The data set employed to generate the plot contains about 2000 individual observations, which do not include observations taken at small solar elongations (i.e., $\varepsilon \leq 5$ degree) to avoid the confusion caused by the side lobe of the Sun. Each point on this plot represents the average of nearly 10 to 15 consecutive observations taken around an epoch and the vertical bar corresponds to $\pm 1 \sigma$ error of each flux density measurement. In the case of the years 1989, 1998, 1999, and 2002, the available number of observations is limited to only about 10 and their average is plotted. However for the later years, each group of plotted points has been derived from about 100 to 200 individual observations.

The weighted average flux density of J1415+1320 for the entire period is 2.70 ± 0.02 Jy, where the weights are taken as the inverse of the square of uncertainties of the flux density measurements. The weighted standard deviation, σ , of flux density variation over epoch is 0.26 Jy. The flux density remains constant through out the observed period except for two epochs around 2008 and 2009, where there is a significant ($> 5\sigma$) excess in the

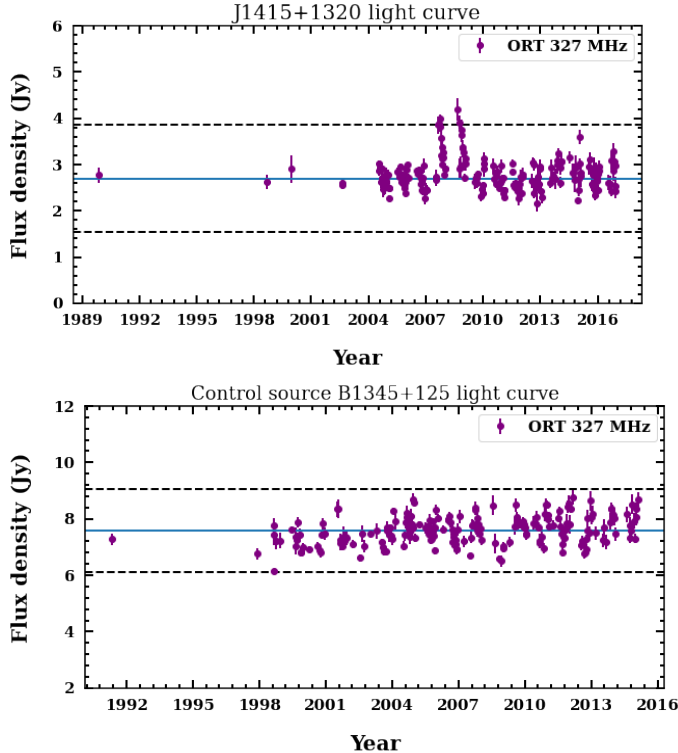


Figure 2. *Top:* 327 MHz light curve of J1415+1320 obtained from the ORT IPS measurements. The blue solid line is drawn at the weighted average of 2.7 Jy. The black dashed line is the 5σ standard deviation. *Bottom:* 327 MHz light curve of a nearby source observed during the same period. The $\pm 3\sigma$ deviation is shown with dashed lines.

flux density. Flux density variation of a nearby control source B1345+125 monitored during similar time period (Figure 2 bottom) does not show flux density excess suggesting that the flare detected in J1415+1320 is likely real. The fluctuations around the mean comes mostly from the confusion and pointing errors owing to the larger beam of ORT. Figure 3 shows the region of the flare. The flares occur at epochs 2007.6 and 2008.6 where the flux density varied by 1.3 Jy ($\sim 50\%$) and the time scale of this variability is ~ 127 days. Unfortunately, the flux measurements are missing in this crucial region. Nevertheless, we evaluate the reliability of the flare using some of the statistics used in time-series data analysis.

3.1. Variability Analysis

Low frequency variability has been extensively studied and the phenomenon is often attributed to scintillations caused by turbulence in the ISM (Cawthorne & Rickett 1985; Spangler et al. 1989; Mantovani et al. 1990; Ghosh & Rao 1992; Riley 1993; Fiedler et al. 1994; Bondi et al. 1996; Salgado et al. 1999; Gaensler & Hunstead 2000; Minns & Riley 2000; Ofek et al. 2011; Bell et al. 2019;

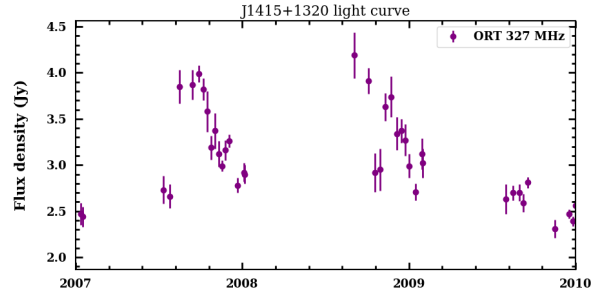


Figure 3. 327 MHz light curve of J1415+1320 covering period between 2007–2010 where a significant excess (flare) is observed.

Ross et al. 2021). The most common techniques that are used to establish low frequency variability in a time series data are –

1. Variability index – defined as the $VI = \sigma/\bar{S}$ where σ is the standard deviation of the flux density over the entire monitoring period, and \bar{S} is the mean flux density. It is a measure of the amplitude of variation with respect to an average value.
2. Structure function (SF) analysis - used to assess variability or constancy of a time series data. For a variable data, it describes the characteristics of variability such as the time scale of variations, or the periodicity in the light curve. It is defined as (following the notation from Spangler et al. (1989))

$$\Sigma(\tau) = \langle (S(t) - S(t + \tau))^2 \rangle \quad (1)$$

where $S(t)$ is the measured flux density at time t , $S(t + \tau)$ is a delayed copy of $S(t)$ by lag time τ , $\langle \cdot \rangle$ is the expected value over time t .

The variability index estimated for J1415+1320 is 8%. The average VI of sources that are found to show significant variability is $\sim 10\%$ (Salgado et al. 1999). The lower VI of J1415+1320 may be indicating variability that is either weak or absent.

We applied the structure function analysis to our 327 MHz time-series data. For non-variable sources, the signal and its delayed copy will be more or less identical and a square of the difference between them displays the variance in the data which is due entirely to measurement errors. Therefore, for non-variable sources, the SF rises from 0 to a saturation value $2\sigma^2$ in within the first few lags. For a variable source, on the other hand, the SF will plateau on a time scale characteristic of the variations and is generally longer than the interval between the observations. We computed a normalized structure

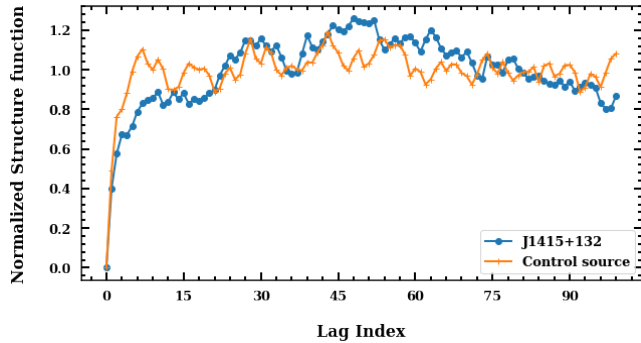


Figure 4. Structure function of J1415+1320 normalized by $2\sigma^2$ for J1415+1320 and the control source B1345+125.

function for both J1415+1320 and the control source B1345+125 by dividing Equation 1 with $2\sigma^2$, where σ^2 is the variance of the measured flux density. Figure 4 shows the normalized SF for these two sources. In the non-variable control source, the SF increases rapidly and flattens within a short lag time. The SF remains constant for any lag. In J1415+1320, the SF shows a two-level structure. It rises gradually when compared to the

control source, approaches a plateau around a lag index of 10 (year 2004.) and then increases around a lag index of 22. Such a structure often indicates contribution from modulating functions that are both intrinsic and extrinsic. A careful look at the structures in the SF and the indices during which they occur seem to be associated with the dense data points around each time period. Therefore, we are unable to comment on any intrinsic or extrinsic variation from the SF.

4. CONCLUSION

We studied the low-frequency multi-epoch data of J1415+1320, a blazar known for its high variability at higher frequencies. The total flux density time series was obtained from the IPS database from the ORT and covers period between 1989 to 2017, although much of the data points exist after 2004. We find a significant variability at two epochs 2008 and 2009. Statistical analysis of this 327 MHz flux density time series provide results that are, however, inadequate to obtain robust estimates of variability properties. Monitoring studies of this source at other low frequencies will be useful in better understanding the low frequency variability.

REFERENCES

- Aller H. D., Aller M. F., Hughes P. A., 1985, *ApJ*, 298, 296
 Bell M. E., et al., 2019, *MNRAS*, 482, 2484
 Bondi M., Padrielli L., Fanti R., Ficarra A., Gregorini L., Mantovani F., 1996, *A&AS*, 120, 89
 Cawthorne T. V., Rickett B. J., 1985, *Nature*, 315, 40
 Fiedler R., Dennison B., Johnston K. J., Waltman E. B., Simon R. S., 1994, *ApJ*, 430, 581
 Gaensler B. M., Hunstead R. W., 2000, *PASA*, 17, 72
 Ghosh T., Rao A. P., 1992, *A&A*, 264, 203
 Manoharan P. K., 2012, *ApJ*, 751, 128
 Manoharan P. K., Subrahmanya C. R., Chengalur J. N., 2017, *Journal of Astrophysics and Astronomy*, 38, 16
 Mantovani F., Fanti R., Gregorini L., Padrielli L., Spangler S., 1990, *A&A*, 233, 535
 Marscher A. P., 2014, *ApJ*, 780, 87
 Marscher A. P., Gear W. K., 1985, *ApJ*, 298, 114
 McHardy I. M., Merrifield M. R., Abraham R. G., Crawford C. S., 1994, *MNRAS*, 268, 681
 Minns A. R., Riley J. M., 2000, *MNRAS*, 315, 839
 Ofek E. O., Frail D. A., Breslauer B., Kulkarni S. R., Chandra P., Gal-Yam A., Kasliwal M. M., Gehrels N., 2011, *ApJ*, 740, 65
 Perlman E. S., Stocke J. T., Shaffer D. B., Carilli C. L., Ma C., 1994, *ApJL*, 424, L69
 Perlman E. S., Carilli C. L., Stocke J. T., Conway J., 1996, *AJ*, 111, 1839
 Qian S. J., Quirrenbach A., Witzel A., Krichbaum T. P., Hummel C. A., Zensus J. A., 1991, *A&A*, 241, 15
 Quirrenbach A., et al., 1992, *A&A*, 258, 279
 Raiteri C. M., et al., 2017, *Nature*, 552, 374
 Readhead A. C. S., et al., 2021, *ApJ*, 907, 61
 Riley J. M., 1993, *MNRAS*, 260, 893
 Ross K., et al., 2021, *MNRAS*, 501, 6139
 Salgado J. F., Altschuler D. R., Ghosh T., Dennison B. K., Mitchell K. J., Payne H. E., 1999, *ApJS*, 120, 77
 Sironi L., Petropoulou M., Giannios D., 2015, *MNRAS*, 450, 183
 Spangler S., Fanti R., Gregorini L., Padrielli L., 1989, *A&A*, 209, 315
 Swarup G., et al., 1971, *Nature Physical Science*, 230, 185
 Vedantham H. K., et al., 2017, *ApJ*, 845, 90
 Werner G. R., Uzdensky D. A., Cerutti B., Nalewajko K., Begelman M. C., 2016, *ApJL*, 816, L8
 Wilkinson P. N., Polatidis A. G., Readhead A. C. S., Xu W., Pearson T. J., 1994, *ApJL*, 432, L87